

# DiffPCN: Latent Diffusion Model Based on Multi-view Depth Images for Point Cloud Completion

Zijun Li<sup>1,3\*</sup>, Hongyu Yan<sup>2\*</sup>, Shijie Li<sup>3</sup>, Kunming Luo<sup>2</sup>, Li Lu<sup>1†</sup>, Xulei Yang<sup>3</sup>, Weisi Lin<sup>4</sup>

<sup>1</sup>Sichuan University

<sup>2</sup>Hong Kong University of Science and Technology

<sup>3</sup>Institute for Infocomm Research (I2R), A\*STAR, Singapore

<sup>4</sup>Nanyang Technological University

## Abstract

Latent diffusion models (LDMs) have demonstrated remarkable generative capabilities across various low-level vision tasks. However, their potential for point cloud completion remains underexplored due to the unstructured and irregular nature of point clouds. In this work, we propose **DiffPCN**, a novel diffusion-based coarse-to-fine framework for point cloud completion. Our approach comprises two stages: an initial stage for generating coarse point clouds, and a refinement stage that improves their quality through point denoising and upsampling. Specifically, we first project the unordered and irregular partial point cloud into structured depth images, which serve as conditions for a well-designed DepthLDM to synthesize completed multi-view depth images that are used to form coarse point clouds. In this way, our DiffPCN can yield high-quality and high-completeness coarse point clouds by leveraging LDM’s powerful generation and comprehension capabilities. Then, since LDMs inevitably introduce outliers into the generated depth maps, we design a Point Denoising Network to remove artifacts from the coarse point cloud by predicting a per-point distance score. Finally, we devise an Association-Aware Point Upsampler, which guides the upsampling process by leveraging local association features between the input point cloud and the corresponding coarse points, further yielding a dense and high-fidelity output. Experimental results demonstrate that our DiffPCN achieves state-of-the-art performance in geometric accuracy and shape completeness, significantly improving the robustness and consistency of point cloud completion.

## Introduction

Point clouds, directly captured by sensors such as LiDAR and depth cameras, provide fundamental 3D spatial information. However, real-world point clouds are often sparse and incomplete due to occlusion, sensor noise, and limited resolution, adversely affecting downstream 3D tasks (Ben-Shabat, Lindenbaum, and Fischer 2018; Qiu, Anwar, and Barnes 2021; Landrieu and Simonovsky 2018; Tang et al. 2022; Rajathi et al. 2023). Therefore, Point cloud completion is proposed aiming to reconstruct dense, structurally coherent point clouds from partial observations, significantly improving 3D perception and reasoning.

\*These authors contributed equally.

†Corresponding author.

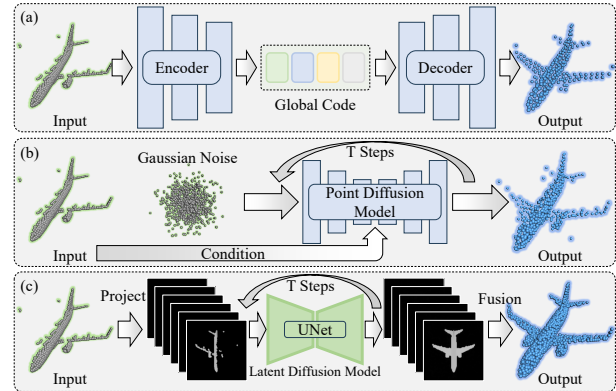


Figure 1: The first stage of mainstream point cloud completion approaches. They are (a): point based methods, (b): point diffusion based methods, and (c): our depth diffusion based method respectively. For each baseline, we render the best-performing point-count setting reported in its paper (Zhu et al. 2023; Lyu et al. 2021).

Most existing point cloud completion approaches follow a coarse-to-fine reconstruction pipeline, where an initial coarse completion is first generated and then refined to improve structural details. Recent studies (Chen et al. 2023; Zhou et al. 2022; Li et al. 2023) emphasize that the quality of initial completion crucially impacts the final reconstruction accuracy and detail. An effective and high-quality initial completion should not only be accurate but also capture fine-grained details. Earlier methods (Xiang et al. 2021; Yu et al. 2021; Yan et al. 2022), typically extract a global feature from the partial input and decode it to reconstruct a coarse point cloud, as shown in Figure 1 (a). However, these global feature based methods inadvertently disrupt point cloud’s original spatial structure and suffer from severe information loss, leading to sparse and structurally inconsistent predictions. To address this issue, recent approaches integrate additional cues to enrich the initial generation process. For instance, SVDFormer (Zhu et al. 2023) integrates depth information to provide explicit geometric constraints, and PC-Dreamer (Wei et al. 2024) fuses global features of generated multi-view images and partial point clouds to predict coarse point clouds. Although these methods can improve feature representation by utilizing cross-modality information, they

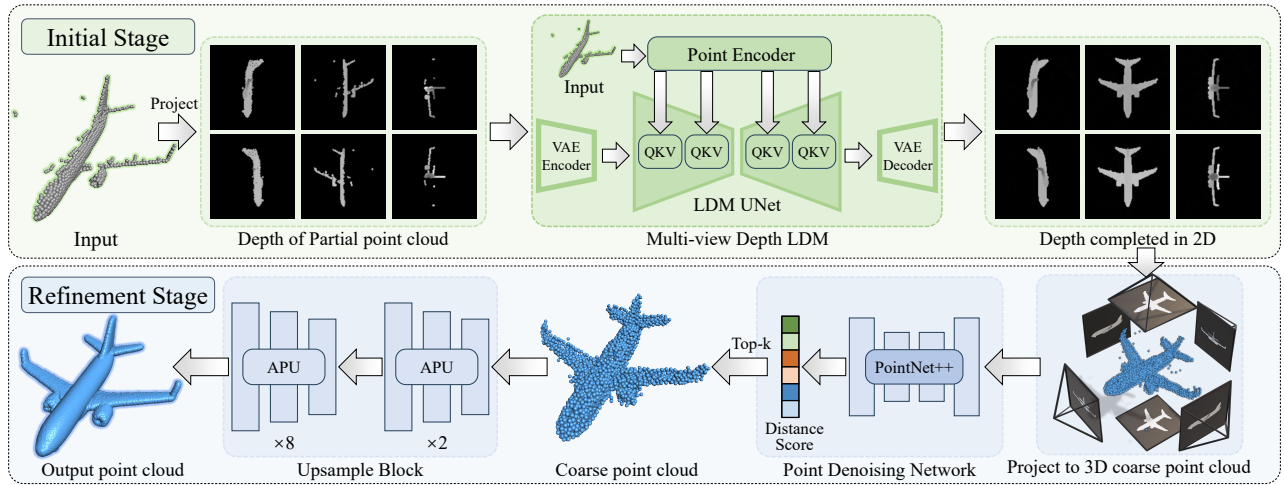


Figure 2: The overall pipeline of DiffPCN. Our DiffPCN consists of two primary stages: the initial stage and refinement stage. The initial stage aims to generate a high-quality initial point clouds from a latent diffusion model based on multi-view depth images from input point clouds. Subsequently, the refinement stage is used to refine and improve the details of the initial point clouds, which is composed of a point denoising network and two stacked association-aware upsampling networks.

still rely on global features to form the initial point cloud, typically no more than 256 points, leading to a failure to capture fine-grained local structures.

Recently, diffusion models (Ho, Jain, and Abbeel 2020; Song, Meng, and Ermon 2020; Ho and Salimans 2022) have demonstrated remarkable success in generating high-quality content. Many low-level tasks (Ke et al. 2024; Nichol et al. 2021; Shiohara and Yamasaki 2024; Kim et al. 2024) also used the diffusion model to solve their problem and achieved impressive performance. Similarly, as shown in Figure 1 (b), some completion methods (Lyu et al. 2021; Chen et al. 2024) also tried to utilize the diffusion model to directly generate coarse point clouds conditional on partial input. However, because these methods directly construct the diffusion model in the 3D space rather than the latent space, they face the efficiency problem. In addition, the irregularity and disorder of point clouds hinder the effectiveness of the diffusion model that works well in continuous representations, such as the image (Rombach et al. 2022; Saharia et al. 2022a), video (Ho et al. 2022; Khachatriyan et al. 2023), and grid (Li et al. 2024). Therefore, they still fail to efficiently synthesize geometrically faithful coarse point clouds, which undermines the entire coarse-to-fine pipeline.

To address the irregularity of raw point sets and harness the robust generalization of latent diffusion model, we introduce DepthLDM, a conditional LDM built on structured multi-view depth images as shown in Figure 1 (c). Inspired by MVDD (Wang et al. 2024), which uses DDPM for unconditional multi-view depth images generation, we first project the unordered input into continuous multi-view depth images. Conditioned on the 2D features of multi-view incomplete depth maps and the 3D features extracted from raw 3D partial point clouds, DepthLDM can generate multi-view consistent depth images to get a high-quality coarse point cloud by leveraging cross-view attention introduced in Wonder3D (Long et al. 2024) and specialized point-aligned at-

tention that can enhance the LDM’s structural consistency and space comprehension. Then, we form the coarse point clouds by directly projecting the depth map back to 3d space. As a result, we can yield more complete and accurate coarse point clouds than the previous methods.

Based on DepthLDM, we introduce a novel coarse-to-fine pipeline for point cloud completion, called **DiffPCN**, as shown in Figure 2. After obtaining the coarse point cloud from DepthLDM, further denoising is required to address artifacts introduced during reconstruction from generated depth images. These artifacts deviate from the object’s boundaries often lead to abnormal points in coarse point cloud (Ke et al. 2024). To mitigate this issue, we introduce the Point Denoising Network (PDNet), which learns to estimate the distance score for each point in coarse point cloud. Using this estimated score, we apply a top-k algorithm to remove points with the highest distance scores, ensuring a more structured and clearer initial point cloud.

Finally, following previous coarse-to-fine pipelines (Xiang et al. 2021; Zhou et al. 2022; Rong et al. 2024), we refine the initial outputs with our Association-Aware Point Upsampler (APU). Since the input point cloud is the sole repository of object texture and detail information, our key insight in designing the APU was to learn the local displacement association between the partial input and the coarse prediction. APU operates in two stages: first, an Association Transformer extracts high-frequency deformation cues by learning the corrective transformation between reliable partial input with its corresponding subset of the coarse prediction; Second, these learned cues are diffused into the full initial point cloud through a cross-attention layer and propagated globally via successive self-attention blocks. This association-driven upsampling yields a dense, geometrically faithful final point cloud that reconstruct both global structure and fine local details.

To validate the effectiveness of our proposed DiffPCN,

we conduct extensive experiments on multiple benchmark datasets, including PCN (Yuan et al. 2018), ShapeNet55/34 dataset (Yu et al. 2021) and MVP dataset (Pan et al. 2021). Our method outperforms existing state-of-the-art approaches in both quantitative metrics and qualitative results, demonstrating superior completeness and structural fidelity. Our main contributions are summarized as follows:

- We propose a novel framework, DiffPCN, to introduce the latent diffusion model for point cloud completion, which achieves state-of-the-art performance on multiple completion benchmarks.
- We propose DepthLDM to transfer the 3D point cloud into the multi-view depth images to inherit the LDM’s powerful generation ability to generate high-quality initial point clouds.
- We propose a point denoising network (PDNet) to remove the outliers by computing the confidence score, as well as designing an association-aware point upsampler (APU) to obtain fine-grained complete point clouds by leveraging the association relation between partial and coarse point clouds.

## Related Work

### Point-based Methods

The introduction of PointNet and PointNet++ (Qi et al. 2017a,b) marked a significant breakthrough in the field of point cloud processing. Based on this, a pioneering method PCN (Yuan et al. 2018) proposed a coarse-to-fine pipeline and a folding-based upsampling block to refine coarse point clouds. Subsequent methods (Wang, Ang Jr, and Lee 2020; Yang et al. 2018; Tchapmi et al. 2019; Pan et al. 2021) extended this idea to further improve performance by leveraging multi-scale local feature extractors and encoder-decoder architectures. Compared to traditional grid-based methods, PointNet-based approaches significantly reduce computational complexity and handle sparse point clouds more effectively (Aoki et al. 2019). However, challenges remain in capturing intricate geometries and global structures. Inspired by the powerful attention machine in transformers, PoinTr (Yu et al. 2021) initiated a new wave of research, which was subsequently advanced by several work (Xiang et al. 2021; Zhu et al. 2023; Yan et al. 2022). Other methods (Chen et al. 2023; Zhou et al. 2022; Zhang et al. 2022) modeled regional discrimination by learning a set of anchors or patches through self-attention. Furthermore, inspired by advances in image-based recognition (Choy et al. 2016; Wei, Yu, and Sun 2022; Yang and Wang 2019), view-guided completion methods (Zhang et al. 2021; Aiello, Valsesia, and Magli 2022; Zhu et al. 2023) were designed to leverage 2D CNNs or ViTs (Liu et al. 2021) to inject the global feature of RGB or depth image into point clouds. Despite the improvements, the model’s inherent limitations in understanding 3D shapes constrain its ability to generate initial point clouds with rich details and logical structures.

### Diffusion-based Methods

As a new generation of generative models, diffusion probabilistic model (Ho, Jain, and Abbeel 2020) has garnered

significant attention since its introduction. It leverages a Markov chain to transform the noise distribution into the data distribution. Subsequent research has explored various aspects (Song, Meng, and Ermon 2020; Luo et al. 2023; Ho and Salimans 2022), greatly enhancing the practicality and efficiency of diffusion models. As a result, diffusion models have been successfully applied to many downstream tasks (Ho et al. 2022; Saharia et al. 2022b; Ke et al. 2024; Nichol et al. 2022; Luo and Hu 2021), achieving excellent performance across diverse domains.

In the field of 3D point cloud completion, diffusion models have demonstrated promising potential, offering new opportunities to address the challenges of conditional shape reconstruction and semantic consistency. PDR (Lyu et al. 2021) is the first work to utilize diffusion model for point cloud completion. It employs DDPM (Song, Meng, and Ermon 2020) and PointNet++ (Qi et al. 2017b) to generate a coarse completion conditioned on partial observations. PointLDM (Chen et al. 2024) further advances this direction by leveraging a coarse-to-fine PointVAE to refine the initial point cloud. However, due to the irregular and unordered nature of point clouds, VAE and diffusion models in the point cloud domain often struggle to achieve optimal performance. Recent work PCDreamer (Wei et al. 2024) harnesses large multi-view diffusion models (Shi et al. 2023; Long et al. 2024) to generate novel views of RGB images for partially observed shapes, using the feature extract from them to predict initial coordinates. While this approach effectively leverages the prior knowledge of 3D space provided by foundation model, it suffers from extremely high computational complexity and relatively low information utilization because they still follow the paradigm of using the global feature to generate a coarse point cloud. In a word, existing diffusion-based methods for point cloud completion face common challenges, inefficient global feature utilization, high computational cost, and difficulty in capturing fine-grained structures from disorder point clouds, which limit their reconstruction quality and scalability.

### Preliminary

Diffusion models have emerged as powerful generative frameworks, demonstrating remarkable performance across diverse modalities such as images, audio, and 3D data (Ho, Jain, and Abbeel 2020; Dhariwal and Nichol 2021; Li et al. 2024). The core idea is to progressively map a data distribution to Gaussian noise through a forward process, then learn to reverse this transformation to generate new samples from gaussian noise. Given a data sample  $x_0$ , the forward process adds Gaussian noise at each step:

$$q(x_t | x_{t-1}) = \mathcal{N}(x_t; \sqrt{\alpha_t}x_{t-1}, (1 - \alpha_t)\mathbf{I}), \quad (1)$$

where  $\alpha_t$  controls the noise level. After sufficiently many steps ( $t = T$ ), the distribution degenerated to an isotropic gaussian. To recover  $x_0$ , a neural network is trained to approximate the reverse process, parameterized as:

$$p_\theta(x_{t-1} | x_t, y) = \mathcal{N}(x_{t-1}; \mu_\theta(x_t, t, y), \Sigma_\theta(t)), \quad (2)$$

where  $y$  represents conditioning information such as class labels (Ho and Salimans 2022), text embeddings (Ramesh

et al. 2022), or structural priors (Nichol et al. 2022). The model minimizes the reconstruction error under conditioning:

$$\mathcal{L} = \mathbb{E}_{x_0, \epsilon, t} \left[ \|\epsilon - \epsilon_\theta(x_t, t, y)\|_2^2 \right], \quad (3)$$

where  $\epsilon$  is the added noise, and  $\epsilon_\theta$  is the noise predictor which is usually UNet structure. Conditional diffusion models enhance control over generation and have shown strong performance in several tasks (Ke et al. 2024; Zhang et al. 2024).

## Method

### Overview

In this section, we introduce DiffPCN, a coarse-to-fine diffusion-based framework for point cloud completion. As illustrated in Figure 2, DiffPCN consists of two primary stages: the initial stage and the refinement stage. The initial stage aim to generate a coarse point cloud, while the refinement stage focuses on improving the quality of coarse point clouds.

### Initial Stage

In this stage, we aim to generate a reliable and detailed initial point cloud. To achieve this, we project the point cloud into the 2D depth image and propose a depth-based latent diffusion model **DepthLDM**, as shown in the upper half of Figure 2.

Specifically, we first train a Variational Autoencoder (VAE) on depth maps projected from ground truth point clouds. For each point cloud, we render 6 views depth images with  $128 \times 128$  resolution by using pre-defined camera poses, including front, back, left, right, up, and down. Similar to Stable Diffusion (Rombach et al. 2022), our VAE comprises an encoder, a KL regularization block, and a decoder. Specifically, given an input depth map  $I \in \mathbb{R}^{H \times W \times 1}$ , it will be encoded as a latent code  $Z \in \mathbb{R}^{H' \times W' \times C}$  which will be further reconstructed into depth image  $I'$  by decoder:

$$z = KL(\mathcal{E}(I)), I' = \mathcal{D}(z) \quad (4)$$

Where  $KL$  indicates KL regularization.  $\mathcal{E}$ ,  $\mathcal{D}$  is our encoder and decoder. We trained the depth VAE following the standard approach and define the losses as:

$$\mathcal{L}_{vae} = \text{MSE}(I_{\text{out}}, I') + \lambda L_{kl}(p(z, I'), \mathcal{N}(0, I)), \quad (5)$$

Then, we build a conditional diffusion model to generate depth images from noise. In practice, we observe that generating each view independently with a diffusion model leads to view inconsistency, resulting in low-quality initial point clouds. To address this issue and improve multi-view consistency, we adopt a cross-view attention mechanism, following Wonder3D (Long et al. 2024). While 2D cross-view attention effectively enforces consistency across different views, it lacks explicit 3D spatial awareness, which can still cause incorrect shape generation (see Sec.?? in the supplementary material). For that reason, to enhance the model’s overall perception of 3D structures, we introduce an additional point-align attention mechanism.

Specifically, in addition to using the latent partial representation  $z_{mv}$  from the VAE-encoded multi-view incomplete depth image  $I_{in}$ , which serves as the primary condition concatenated with the input noise  $x_{mv}$ , we apply a point-align cross attention to incorporate the spatial feature  $f_c$  of the partial point cloud as the additional condition. This allows us to generate semantic consistency and reliable multi-view latents  $\hat{z} = \{z_1, z_2, \dots, z_m\}$ , where  $m$  is the number of generated views. To extract the 3d structural point features, we use a pretrained Point-Bert (Yu et al. 2022) as the point encoder to sample the points and extract patch-wise feature tokens, and concatenate the 2D coordinates of each point relative to every 2D view to align 2D and 3D domain, further form structural condition  $f_c$ . This additional condition, which encodes high-dimensional structural information, enhances the DepthLDM’s perception of 3D space through the cross attention mechanism, thereby further improving the object structural consistency.

Finally, completed multi-view depth images can be obtained from those latents through VAE decoding, and the UNet  $\epsilon_\theta$  is trained as follows:

$$\mathcal{L}_{MVD} = \mathbb{E}_{x_0, \epsilon, t} \left[ \|\epsilon_{mv} - \epsilon_\theta(x_{mv}, z_c, t, f_c)\|_2^2 \right], \quad (6)$$

where  $x_{mv}$  is the noisy sample of  $z_{mv}$ ,  $t$  is the time steps and  $f_c$  is the point perception feature from Point-Bert.

### Refinement Stage

In this stage, we aim to refine coarse point clouds formed from the initial stage. As illustrated in the bottom of Figure 2, it begins by using a Point Denoising Network to remove the abnormal points introduced from the first stage. Then, an association relation construction module is utilized to learn a local transfer association from the reliable input structure to the corresponding coarse prediction. Finally, we stack two Association-Aware Point Upsamplers that propagate this association feature to the entire initial point cloud, further obtain the final complete point cloud.

**Point Denoising Network** Inevitable, the UNet tends to generate erroneous values in regions with large gaps (Ran, Guizilini, and Wang 2024; Ke et al. 2024). Therefore, at the object boundaries in the generated depth maps, DepthLDM introduces some outliers, which, after projection, manifest as noise that adversely affects the subsequent upsampling process. Therefore, the Point Denoising Network (PDNet) is designed to identify and remove those abnormal points that deviate significantly from the object boundaries. To achieve this, the network learns to estimate the minimum distance between each point and the ground truth point cloud.

Specifically, as shown in Fig. 2, our PDNet consists of an UNet-based feature extractor built by PointNet++ (Qi et al. 2017b) and an MLP-based prediction head. Given a coarse point cloud  $P_c \in \mathbb{R}^{N_c \times 3}$ , our feature extractor utilizes a multi-scale mechanism to compute the point’s position feature  $F_c \in \mathbb{R}^{N_c \times C_c}$  by considering the global coordinate distribution. Then, the prediction head is employed to directly predict the distance score  $d_{pre} \in \mathbb{R}^{N_c \times 1}$  for each point.

We use the single-sided chamfer distance between the coarse point cloud and the ground truth point cloud as the

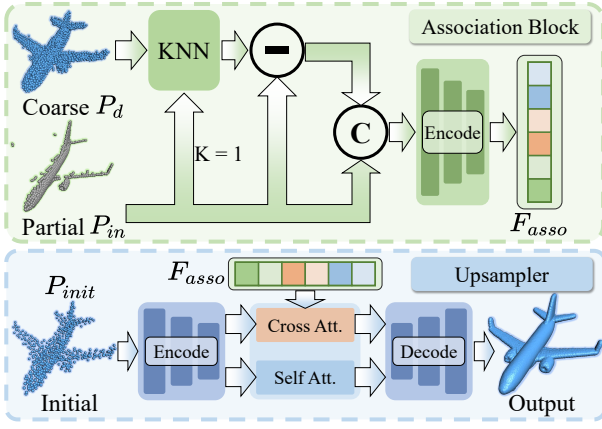


Figure 3: The overall structure of our Association Point Upsampler. “-” and “c” represent the subtraction and concatenate operation respectively.

ground truth distance. This value serves as the supervisory signal for training the PDNet, which can be formulated as:

$$\mathcal{L}_r = \text{MSE}(\mathcal{D}_\theta(P_c), D_{gt}) \quad (7)$$

where  $\mathcal{D}_\theta$ ,  $P_c$ , and  $D_{gt}$  are our learnable distance estimation network, input coarse point cloud generated by DepthLDM, and ground truth distance, respectively. After the training, the network can adaptively predict the distance value of each point from the coarse point clouds.

Once the minimal distances  $d_{pre}$  have predicted, we use the top-k algorithm to filter the abnormal points to get the denoised point cloud  $P_d \in \mathbb{R}^{N_d \times 3}$ . Finally, following previous completion methods (Yan et al. 2022; Xiang et al. 2021), we further merge  $P_d$  with the input partial point cloud  $P_{in}$  and sample to  $N_i$  points by the farthest point sampling (FPS), forming the final initial point cloud  $P_{init} \in \mathbb{R}^{N_i \times 3}$ .

**Association Relation Construction.** While the PDNet effectively removes abnormal points and provides a reliable initial point cloud, achieving high-resolution and structurally accurate reconstructions still requires further refinement. To address this, we initially introduce an association mechanism to extract the general transform feature.

As shown in Figure 3, given the partial input  $P_{in} \in \mathbb{R}^{N_p \times 3}$  and the denoised coarse point cloud  $P_d \in \mathbb{R}^{N_d \times 3}$ , it begin with extracting a geometrically matched subset by a 1-nearest-neighbor lookup:

$$P_{asso} = \text{KNN}(P_d, P_{in}, k = 1) \quad (8)$$

where we set k to 1 for getting unique neighbors, and  $P_{asso}$  aligns exactly with its corresponding observed point in  $P_{in}$ .

Since PointLDM inevitably introduces some reconstruction error, and  $P_{in}$  is taken from the ground-truth coordinates, we compute the point-wise residual  $\Delta P_{asso} = P_{in} - P_d$  as a measure of the correlation tendency between the reconstructed coordinates and the ground truth. We then employ an association encoder to obtain these association features that are used in the subsequent upsampling process.

Considering that these association features fundamentally learn a generalizable correction scheme, we cannot simply

confine their encoding to either the coordinate domain or the feature domain. To address this, we propose a novel association encoder that operates in parallel, incorporating both a Point Transformer (Zhao et al. 2021) and a EdgeConv module (Wang et al. 2019). Detailed specifications of this encoder can be found in the Supplementary.

**Association-Aware Point Upsampler** The Association-Aware Point Upsampler completes the refinement process by propagating the learned association features  $F_{asso}$  into every point of the initial point cloud. It begins by encoding  $P_{init}$  with a common point encoder which consists mainly of a point transformer and a self-attention block into high-dimensional features  $F_m \in \mathbb{R}^{N_m \times C_m}$ .

Next, we inject the local association feature via cross-attention, using  $F_m$  as queries and  $F_{asso}$  as keys and values. To preserve residual detail from the initial point cloud, we simultaneously apply a parallel self-attention branch to the original features  $F_m$ . We then concatenate these two streams along the channel dimension, and feed into a lightweight decoder  $\mathcal{D}_p$  following SVDFormer (Zhu et al. 2023), which is composed of two self-attention layers interleaved with MLPs. The whole module can be formulated as:

$$F_o = \mathcal{D}_p([\text{SA}(F_m), \text{CA}(F_m, F_{asso})]) \quad (9)$$

Finally, following the point-shuffle operation (Yang et al. 2018), we scatter the regressed offsets onto repeated copies of each coarse point, yielding the dense, high-fidelity upsampled cloud.

**Loss Function** For the refinement stage, we use the Chamfer Distance (CD) as the main distance function, which measures the average of the closest point distances between the output and the ground truth. The end-to-end loss function is formulated as:

$$\mathcal{L}_{refine} = \mathcal{L}_r + \sum_{i=1}^n \mathcal{L}_{CD}(P_o^i, Q), \quad (10)$$

where  $\mathcal{L}_r$  corresponds to the PDNet loss, the second term is the total loss of our APU.  $Q$  is the ground truth point cloud,  $P_o^i$  denote the final output of each APU, and  $n$  is the stacked number of APU we used.

## Experiments

In this section, we begin by introducing the datasets and evaluation metrics used for the point cloud completion tasks. Then, we compare our method with previous state-of-the-art approaches. Finally, we present an ablation study of our model.

### Datasets and Evaluation Metrics

**PCN’s dataset:** PCN’s dataset (Yuan et al. 2018) is a subset of ShapeNet. It consists of 28,974 training samples and 1,200 test samples from 8 categories, which is widely used as a benchmark for 3D point cloud completion. **MVP dataset:** The MVP dataset (Pan et al. 2021) includes 4,000 samples across 16 categories. Each model is virtually scanned from 26 camera positions, simulating realistic multi-view observations and better reflecting real-world

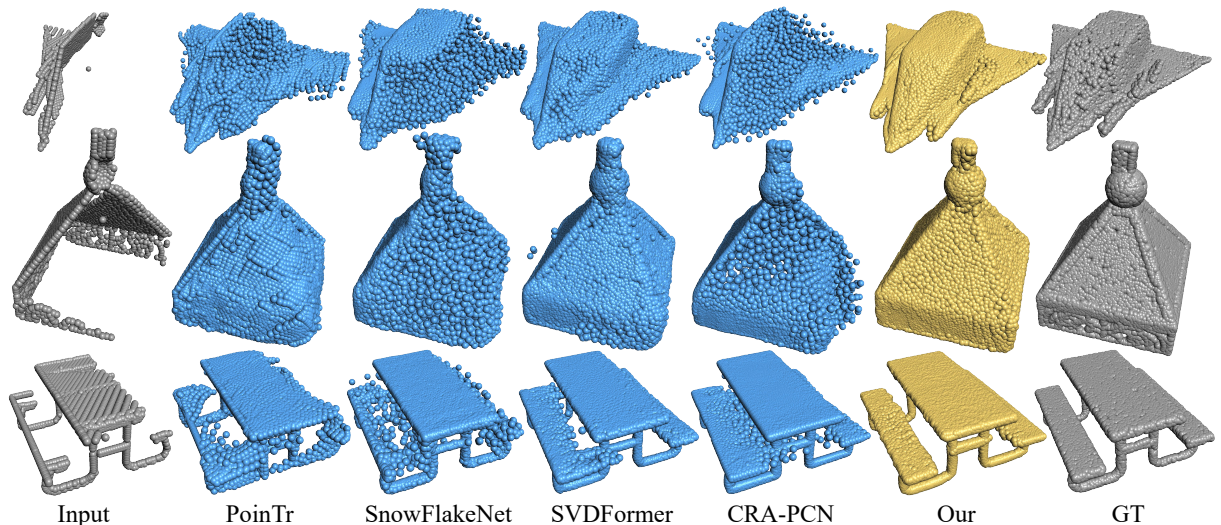


Figure 4: Visualization on the PCN’s dataset. Our DiffPCN presents a better performance compared with previous methods.

Methods	Airplane	Cabinet	Car	Chair	Lamp	Sofa	Table	Watercraft	CD <sub>avg</sub> (↓)	F1 (↑)
PoinTr (Yu et al. 2021)	4.75	10.47	8.68	9.39	7.75	10.93	7.78	7.29	8.38	-
SnowflakeNet (Xiang et al. 2021)	4.29	9.16	8.08	7.89	6.07	9.23	6.55	6.40	7.21	0.801
FBNet (Yan et al. 2022)	3.99	9.05	7.90	7.38	5.82	8.85	6.35	6.18	6.94	-
SVDFormer (Zhu et al. 2023)	3.62	8.79	7.46	6.91	5.33	8.49	5.90	5.83	6.54	0.841
PCDreamer (Wei et al. 2024)	3.51	8.72	6.89	6.71	5.64	8.32	6.24	5.84	6.49	<u>0.856</u>
CRA-PCN (Rong et al. 2024)	3.59	8.70	7.50	6.70	<u>5.06</u>	8.24	5.72	5.64	6.39	-
PointCFormer (Zhong et al. 2025)	3.53	8.73	7.32	6.68	5.12	8.34	5.86	5.74	6.41	0.855
SymmCompletion (Yan et al. 2025)	<u>3.53</u>	<b>8.49</b>	7.30	<u>6.52</u>	<u>5.06</u>	8.23	<b>5.64</b>	<b>5.49</b>	<u>6.28</u>	0.853
<b>DiffPCN</b>	<b>3.49</b>	<u>8.52</u>	<b>7.26</b>	<b>6.51</b>	<b>4.90</b>	<b>8.15</b>	<u>5.69</u>	<b>5.49</b>	<b>6.25</b>	<b>0.858</b>

Table 1: Quantitative results in terms of  $l1$  Chamfer Distance  $\times 10^3$  (CD) and F1-Score@%1 (F1) on PCN’s dataset.

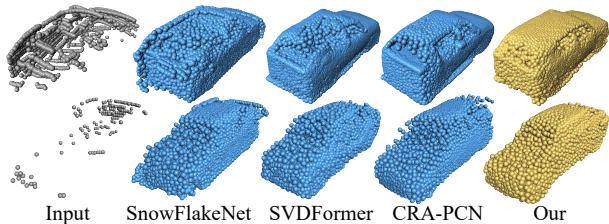


Figure 5: Visual comparisons on the KITTI dataset.

variations in perspective. **KITTI**: KITTI (Geiger et al. 2013) is a real-world dataset consist of 2,400 LiDAR-scanned car point clouds provided only as a test set, without fine registration. As models must be trained on other datasets and evaluated directly on these unaligned scans, KITTI poses a rigorous benchmark for assessing generalization and robustness in practical applications.

**Evaluation Metrics**: Similar to the previous methods (Yuan et al. 2018; Yu et al. 2021; Xiang et al. 2021), we adopt Chamfer distance (CD) and F1 score as our main metrics. For KITTI dataset, we use Minimal Matching Distance (MMD) and Fidelity (FD) to evaluate the performance.

## Experiment Results

Initially, We evaluate our performance on the PCN’s dataset. Table 1 and 4 shows that DiffPCN establishes new state-of-the-art results on PCN, achieving the lowest CD and highest F1. Qualitatively, the airplane in the first row illustrates how APU extends observed wing surfaces into unobserved regions, producing a smooth, high-fidelity reconstruction. The lamp in the second row demonstrates that PDNet effectively removes spurious points to yield a clean, noise-free completion. Finally, the bench in the third row showcases DepthLDM’s multi-view understanding, reconstructing intricate structures with precise geometric detail. These results demonstrate that DiffPCN, benefiting from the proposed modules, achieves more realistic and clear completions, ultimately reaching state-of-the-art performance. We further evaluate our model on the MVP dataset across all resolutions (2K, 4K, 8K, and 16K). The quantitative results, shown in Table 2, indicate that our method consistently achieves the best performance under different densities, which effectively shown the robustness of our diffusion-based method.

Finally, we test our model on the KITTI dataset. Following previous methods (Zhu et al. 2023; Rong et al. 2024), we use the pre-trained model trained on the PCN dataset for evaluation. The quantitative comparison is presented below:

Method	2048		4096		8192		16384	
	CD ( $\downarrow$ )	F1 ( $\uparrow$ )	CD ( $\downarrow$ )	F1 ( $\uparrow$ )	CD ( $\downarrow$ )	F1 ( $\uparrow$ )	CD ( $\downarrow$ )	F1 ( $\uparrow$ )
PCN (Yuan et al. 2018)	9.77	0.320	7.96	0.458	6.99	0.563	6.02	0.638
VRCNet (Pan et al. 2021)	5.96	0.499	4.70	0.636	3.64	0.727	3.12	0.791
SnowflakeNet (Xiang et al. 2021)	5.71	0.503	4.40	0.661	3.48	0.743	2.73	0.796
PDR (Lyu et al. 2021)	5.66	0.499	4.26	0.649	3.35	0.754	2.61	0.817
FBNet (Yan et al. 2022)	5.06	0.532	3.88	0.671	2.99	0.766	2.29	0.822
AEDNet (Fu et al. 2024)	5.12	0.522	3.75	0.675	2.90	0.770	2.24	0.832
SymmCompletion (Yan et al. 2025)	<b>4.89</b>	<u>0.534</u>	<u>3.65</u>	<b>0.691</b>	<u>2.70</u>	<u>0.782</u>	<u>2.14</u>	<u>0.850</u>
<b>DiffPCN</b>	<b>4.89</b>	<b>0.536</b>	<b>3.63</b>	<u>0.690</u>	<b>2.68</b>	<b>0.791</b>	<b>2.06</b>	<b>0.857</b>

Table 2: Quantitative results in terms of L2 Chamfer Distance  $\times 10^4$  (CD) and F1-score@%1 (F1) on the MVP dataset with different resolutions.

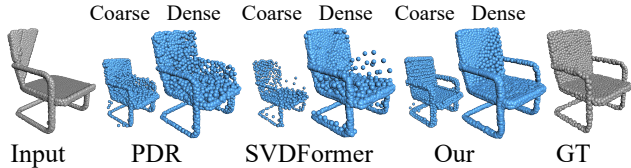


Figure 6: Visual comparisons of initial stage on MVP2K dataset.

Methods	SVDFormer	CRA-PCN	Symm	DiffPCN
FD ( $\downarrow$ )	1.28	1.96	2.54	<b>1.09</b>
MMD ( $\downarrow$ )	0.75	1.08	1.72	<b>0.61</b>

Our method achieves the best results in both MMD and FD, surpassing all previous state-of-the-art methods. This strong performance stems from the high generalization capability of our diffusion-based DepthLDM: even on unprocessed LiDAR scans with variable point densities, DiffPCN produces reliable coarse predictions and robust refinements. Additionally, the qualitative results in Figure 5 demonstrate that our approach consistently achieves superior completeness. Notably, our model outperforms all existing methods across different scenarios, whether in relatively simple cases with denser input points or in more challenging cases with extremely sparse inputs.

## Ablation Study

**The effectiveness of DepthLDM.** To validate the effectiveness of the depth latent diffusion model for the initial stage, we compare our DepthLDM with previous methods. Specifically, within our framework, we replace DepthLDM with the coarse point cloud generation methods from these approaches, including point-based SVDFormer (Zhu et al. 2023) and diffusion-based PDR (Lyu et al. 2021). Since PDR only provides a pre-trained model on the MVP dataset, we conduct this comparison using the MVP dataset. As shown in Table 3, our DepthLDM achieves the best performance, demonstrating its ability to generate a high-quality initial point cloud. We also provide qualitative comparisons in Figure 6. In the initial stage, PDR and SVDFormer struggle to generate high-quality complete initial point clouds, which further affects the final quality for the refinement stage. In contrast, our model generates a structurally accurate initial point cloud, ultimately achieving the best final

Initial Generator	CD ( $\downarrow$ )	F1 ( $\uparrow$ )
PDR (Lyu et al. 2021)	5.21	0.519
SVDFormer (Zhu et al. 2023)	5.68	0.498
<b>DepthLDM (Ours)</b>	<b>4.89</b>	<b>0.536</b>

Table 3: Quantitative comparison between different coarse point cloud generation (initial stage) methods on MVP2K.

Upsampler $F_k$	CD ( $\downarrow$ )	F1 ( $\uparrow$ )
SPD (Xiang et al. 2021)	6.96	0.811
SDG (Zhu et al. 2023)	6.45	0.846
<b>APU (Ours)</b>	<b>6.25</b>	<b>0.858</b>

Table 4: Quantitative comparison about our APU on PCN dataset (Yuan et al. 2018)

results.

**The effectiveness of APU.** To quantify the impact of our upsampler, we replace the full APU with other upsampler from sota methods and test on the PCN dataset. As Table 4 shows, compared to the classical refiner SPD (Xiang et al. 2021), our APU achieves a significant improvement in both the CD and F1 scores, confirming its superior reconstruction fidelity. In addition, compared to the SGD (Zhu et al. 2023) that also introduces the features of partial input via a cross-attention layer, our Association-Transformer provides unique displacement trend information, ultimately achieving superior results. These results validate that our association-aware feature encoding and fusion strategy are key to generating dense and accurate point clouds.

## Conclusion

In this paper, we propose DiffPCN, a novel depth diffusion-based coarse-to-fine framework for point cloud completion. By transforming 3D unordered point cloud into a 2D structured depth image, our approach leverages DepthLDM to generate a completed multi-view depth image with more details and project it to form a coarse point cloud. To remove the outlier points in the coarse point cloud, we design a Point Denoising Network to predict the confidence score and leverage the Top-K algorithm to choose high-confidence points. Further on, we stack two Association-Aware Point Upsamplers to progressively refine initial point clouds by introducing the association features. Extensive experiments on

benchmark datasets demonstrate that DiffPCN outperforms existing methods both in geometric accuracy and completeness, highlighting the effectiveness of leveraging 2D LDMs for high-quality 3D reconstruction.

## References

- Aiello, E.; Valsesia, D.; and Magli, E. 2022. Cross-modal learning for image-guided point cloud shape completion. *Advances in Neural Information Processing Systems*, 35: 37349–37362.
- Aoki, Y.; Goforth, H.; Srivatsan, R. A.; and Lucey, S. 2019. Pointnetlk: Robust & efficient point cloud registration using pointnet. In *Proceedings of the IEEE/CVF conference on computer vision and pattern recognition*, 7163–7172.
- Ben-Shabat, Y.; Lindenbaum, M.; and Fischer, A. 2018. 3dmfv: Three-dimensional point cloud classification in real-time using convolutional neural networks. *IEEE Robotics and Automation Letters*, 3(4): 3145–3152.
- Chen, Z.; Long, F.; Qiu, Z.; Yao, T.; Zhou, W.; Luo, J.; and Mei, T. 2023. AnchorFormer: Point Cloud Completion From Discriminative Nodes. In *Proceedings of the IEEE/CVF Conference on Computer Vision and Pattern Recognition*, 13581–13590.
- Chen, Z.; Long, F.; Qiu, Z.; Yao, T.; Zhou, W.; Luo, J.; and Mei, T. 2024. Learning 3D Shape Latent for Point Cloud Completion. *IEEE Transactions on Multimedia*.
- Choy, C. B.; Xu, D.; Gwak, J.; Chen, K.; and Savarese, S. 2016. 3d-r2n2: A unified approach for single and multi-view 3d object reconstruction. In *Computer Vision—ECCV 2016: 14th European Conference, Amsterdam, The Netherlands, October 11–14, 2016, Proceedings, Part VIII 14*, 628–644. Springer.
- Dhariwal, P.; and Nichol, A. 2021. Diffusion models beat gans on image synthesis. *Advances in neural information processing systems*, 34: 8780–8794.
- Fu, Z.; Wang, L.; Xu, L.; Wang, Z.; Laga, H.; Guo, Y.; Boussaid, F.; and Bennamoun, M. 2024. AEDNet: Adaptive Embedding and Multiview-Aware Disentanglement for Point Cloud Completion. In *European Conference on Computer Vision*, 127–143. Springer.
- Geiger, A.; Lenz, P.; Stiller, C.; and Urtasun, R. 2013. Vision meets robotics: The kitti dataset. *The International Journal of Robotics Research*, 32(11): 1231–1237.
- Ho, J.; Jain, A.; and Abbeel, P. 2020. Denoising diffusion probabilistic models. *Advances in neural information processing systems*, 33: 6840–6851.
- Ho, J.; and Salimans, T. 2022. Classifier-free diffusion guidance. *arXiv preprint arXiv:2207.12598*.
- Ho, J.; Salimans, T.; Gritsenko, A.; Chan, W.; Norouzi, M.; and Fleet, D. J. 2022. Video diffusion models. *Advances in Neural Information Processing Systems*, 35: 8633–8646.
- Ke, B.; Obukhov, A.; Huang, S.; Metzger, N.; Daudt, R. C.; and Schindler, K. 2024. Repurposing diffusion-based image generators for monocular depth estimation. In *Proceedings of the IEEE/CVF Conference on Computer Vision and Pattern Recognition*, 9492–9502.
- Khachatryan, L.; Movsisyan, A.; Tadevosyan, V.; Henschel, R.; Wang, Z.; Navasardyan, S.; and Shi, H. 2023. Text2video-zero: Text-to-image diffusion models are zero-shot video generators. In *Proceedings of the IEEE/CVF International Conference on Computer Vision*, 15954–15964.
- Kim, J.; Gu, G.; Park, M.; Park, S.; and Choo, J. 2024. Stableviton: Learning semantic correspondence with latent diffusion model for virtual try-on. In *Proceedings of the IEEE/CVF conference on computer vision and pattern recognition*, 8176–8185.
- Landrieu, L.; and Simonovsky, M. 2018. Large-scale point cloud semantic segmentation with superpoint graphs. In *Proceedings of the IEEE conference on computer vision and pattern recognition*, 4558–4567.
- Li, S.; Gao, P.; Tan, X.; and Wei, M. 2023. ProxyFormer: Proxy Alignment Assisted Point Cloud Completion with Missing Part Sensitive Transformer. In *Proceedings of the IEEE/CVF Conference on Computer Vision and Pattern Recognition*, 9466–9475.
- Li, W.; Liu, J.; Chen, R.; Liang, Y.; Chen, X.; Tan, P.; and Long, X. 2024. Craftsman: High-fidelity mesh generation with 3d native generation and interactive geometry refiner. *arXiv preprint arXiv:2405.14979*.
- Liu, Z.; Lin, Y.; Cao, Y.; Hu, H.; Wei, Y.; Zhang, Z.; Lin, S.; and Guo, B. 2021. Swin transformer: Hierarchical vision transformer using shifted windows. In *Proceedings of the IEEE/CVF international conference on computer vision*, 10012–10022.
- Long, X.; Guo, Y.-C.; Lin, C.; Liu, Y.; Dou, Z.; Liu, L.; Ma, Y.; Zhang, S.-H.; Habermann, M.; Theobalt, C.; et al. 2024. Wonder3d: Single image to 3d using cross-domain diffusion. In *Proceedings of the IEEE/CVF Conference on Computer Vision and Pattern Recognition*, 9970–9980.
- Luo, S.; and Hu, W. 2021. Diffusion probabilistic models for 3d point cloud generation. In *Proceedings of the IEEE/CVF conference on computer vision and pattern recognition*, 2837–2845.
- Luo, S.; Tan, Y.; Huang, L.; Li, J.; and Zhao, H. 2023. Latent consistency models: Synthesizing high-resolution images with few-step inference. *arXiv preprint arXiv:2310.04378*.
- Lyu, Z.; Kong, Z.; Xu, X.; Pan, L.; and Lin, D. 2021. A conditional point diffusion-refinement paradigm for 3d point cloud completion. *arXiv preprint arXiv:2112.03530*.
- Nichol, A.; Dhariwal, P.; Ramesh, A.; Shyam, P.; Mishkin, P.; McGrew, B.; Sutskever, I.; and Chen, M. 2021. Glide: Towards photorealistic image generation and editing with text-guided diffusion models. *arXiv preprint arXiv:2112.10741*.
- Nichol, A.; Jun, H.; Dhariwal, P.; Mishkin, P.; and Chen, M. 2022. Point-e: A system for generating 3d point clouds from complex prompts. *arXiv preprint arXiv:2212.08751*.
- Pan, L.; Chen, X.; Cai, Z.; Zhang, J.; Zhao, H.; Yi, S.; and Liu, Z. 2021. Variational Relational Point Completion Network. In *Proceedings of the IEEE/CVF Conference on Computer Vision and Pattern Recognition*, 8524–8533.
- Qi, C. R.; Su, H.; Mo, K.; and Guibas, L. J. 2017a. Pointnet: Deep learning on point sets for 3d classification and segmentation. In *Proceedings of the IEEE conference on computer vision and pattern recognition*, 652–660.
- Qi, C. R.; Yi, L.; Su, H.; and Guibas, L. J. 2017b. Pointnet++: Deep hierarchical feature learning on point sets in a metric space. *Advances in neural information processing systems*, 30.

- Qiu, S.; Anwar, S.; and Barnes, N. 2021. Dense-resolution network for point cloud classification and segmentation. In *Proceedings of the IEEE/CVF winter conference on applications of computer vision*, 3813–3822.
- Rajathi, K.; Gomathi, N.; Mahdal, M.; and Guras, R. 2023. Path segmentation from point cloud data for autonomous navigation. *Applied Sciences*, 13(6): 3977.
- Ramesh, A.; Dhariwal, P.; Nichol, A.; Chu, C.; and Chen, M. 2022. Hierarchical text-conditional image generation with clip latents. *arXiv preprint arXiv:2204.06125*, 1(2): 3.
- Ran, H.; Guizilini, V.; and Wang, Y. 2024. Towards realistic scene generation with lidar diffusion models. In *Proceedings of the IEEE/CVF Conference on Computer Vision and Pattern Recognition*, 14738–14748.
- Rombach, R.; Blattmann, A.; Lorenz, D.; Esser, P.; and Ommer, B. 2022. High-resolution image synthesis with latent diffusion models. In *Proceedings of the IEEE/CVF conference on computer vision and pattern recognition*, 10684–10695.
- Rong, Y.; Zhou, H.; Yuan, L.; Mei, C.; Wang, J.; and Lu, T. 2024. Cra-pcn: Point cloud completion with intra-and inter-level cross-resolution transformers. In *Proceedings of the AAAI Conference on Artificial Intelligence*, volume 38, 4676–4685.
- Saharia, C.; Chan, W.; Chang, H.; Lee, C.; Ho, J.; Salimans, T.; Fleet, D.; and Norouzi, M. 2022a. Palette: Image-to-image diffusion models. In *ACM SIGGRAPH 2022 conference proceedings*, 1–10.
- Saharia, C.; Chan, W.; Saxena, S.; Li, L.; Whang, J.; Denton, E. L.; Ghasemipour, K.; Gontijo Lopes, R.; Karagol Ayan, B.; Salimans, T.; et al. 2022b. Photorealistic text-to-image diffusion models with deep language understanding. *Advances in neural information processing systems*, 35: 36479–36494.
- Shi, Y.; Wang, P.; Ye, J.; Long, M.; Li, K.; and Yang, X. 2023. Mvdream: Multi-view diffusion for 3d generation. *arXiv preprint arXiv:2308.16512*.
- Shiohara, K.; and Yamasaki, T. 2024. Face2diffusion for fast and editable face personalization. In *Proceedings of the IEEE/CVF Conference on Computer Vision and Pattern Recognition*, 6850–6859.
- Song, J.; Meng, C.; and Ermon, S. 2020. Denoising diffusion implicit models. *arXiv preprint arXiv:2010.02502*.
- Tang, L.; Zhan, Y.; Chen, Z.; Yu, B.; and Tao, D. 2022. Contrastive boundary learning for point cloud segmentation. In *Proceedings of the IEEE/CVF Conference on Computer Vision and Pattern Recognition*, 8489–8499.
- Tchapmi, L. P.; Kosaraju, V.; Rezatofighi, H.; Reid, I.; and Savarese, S. 2019. Topnet: Structural point cloud decoder. In *Proceedings of the IEEE/CVF Conference on Computer Vision and Pattern Recognition*, 383–392.
- Wang, X.; Ang Jr, M. H.; and Lee, G. H. 2020. Cascaded refinement network for point cloud completion. In *Proceedings of the IEEE/CVF Conference on Computer Vision and Pattern Recognition*, 790–799.
- Wang, Y.; Sun, Y.; Liu, Z.; Sarma, S. E.; Bronstein, M. M.; and Solomon, J. M. 2019. Dynamic graph cnn for learning on point clouds. *Acm Transactions On Graphics (tog)*, 38(5): 1–12.
- Wang, Z.; Xu, Q.; Tan, F.; Chai, M.; Liu, S.; Pandey, R.; Fanello, S.; Kadambi, A.; and Zhang, Y. 2024. Mvdd: Multi-view depth diffusion models. In *European Conference on Computer Vision*, 236–253. Springer.
- Wei, G.; Feng, Y.; Ma, L.; Wang, C.; Zhou, Y.; and Li, C. 2024. PCDreamer: Point Cloud Completion Through Multi-view Diffusion Priors. *arXiv preprint arXiv:2411.19036*.
- Wei, X.; Yu, R.; and Sun, J. 2022. Learning view-based graph convolutional network for multi-view 3d shape analysis. *IEEE Transactions on Pattern Analysis and Machine Intelligence*, 45(6): 7525–7541.
- Xiang, P.; Wen, X.; Liu, Y.-S.; Cao, Y.-P.; Wan, P.; Zheng, W.; and Han, Z. 2021. Snowflakenet: Point cloud completion by snowflake point deconvolution with skip-transformer. In *Proceedings of the IEEE/CVF International Conference on Computer Vision*, 5499–5509.
- Yan, H.; Li, Z.; Luo, K.; Lu, L.; and Tan, P. 2025. Symm-Completion: High-Fidelity and High-Consistency Point Cloud Completion with Symmetry Guidance. In *Proceedings of the AAAI Conference on Artificial Intelligence*, volume 39, 9094–9102.
- Yan, X.; Yan, H.; Wang, J.; Du, H.; Wu, Z.; Xie, D.; Pu, S.; and Lu, L. 2022. Fbnet: Feedback network for point cloud completion. In *Computer Vision—ECCV 2022: 17th European Conference, Tel Aviv, Israel, October 23–27, 2022, Proceedings, Part II*, 676–693. Springer.
- Yang, Y.; Feng, C.; Shen, Y.; and Tian, D. 2018. Foldingnet: Point cloud auto-encoder via deep grid deformation. In *Proceedings of the IEEE Conference on Computer Vision and Pattern Recognition*, 206–215.
- Yang, Z.; and Wang, L. 2019. Learning relationships for multi-view 3D object recognition. In *Proceedings of the IEEE/CVF international conference on computer vision*, 7505–7514.
- Yu, X.; Rao, Y.; Wang, Z.; Liu, Z.; Lu, J.; and Zhou, J. 2021. PointR: Diverse point cloud completion with geometry-aware transformers. In *Proceedings of the IEEE/CVF International Conference on Computer Vision*, 12498–12507.
- Yu, X.; Tang, L.; Rao, Y.; Huang, T.; Zhou, J.; and Lu, J. 2022. Point-bert: Pre-training 3d point cloud transformers with masked point modeling. In *Proceedings of the IEEE/CVF conference on computer vision and pattern recognition*, 19313–19322.
- Yuan, W.; Khot, T.; Held, D.; Mertz, C.; and Hebert, M. 2018. Pcn: Point completion network. In *2018 International Conference on 3D Vision (3DV)*, 728–737. IEEE.
- Zhang, W.; Zhou, H.; Dong, Z.; Liu, J.; Yan, Q.; and Xiao, C. 2022. Point cloud completion via skeleton-detail transformer. *IEEE Transactions on Visualization and Computer Graphics*, 29(10): 4229–4242.
- Zhang, X.; Feng, Y.; Li, S.; Zou, C.; Wan, H.; Zhao, X.; Guo, Y.; and Gao, Y. 2021. View-guided point cloud completion.

In *Proceedings of the IEEE/CVF conference on computer vision and pattern recognition*, 15890–15899.

Zhang, Y.; Zhang, J.; Li, H.; Wang, Z.; Hou, L.; Zou, D.; and Bian, L. 2024. Diffusion-based Blind Text Image Super-Resolution. In *Proceedings of the IEEE/CVF Conference on Computer Vision and Pattern Recognition*, 25827–25836.

Zhao, H.; Jiang, L.; Jia, J.; Torr, P. H.; and Koltun, V. 2021. Point transformer. In *Proceedings of the IEEE/CVF international conference on computer vision*, 16259–16268.

Zhong, Y.; Quan, W.; Yan, D.-M.; Jiang, J.; and Wei, Y. 2025. PointCFormer: A relation-based progressive feature extraction network for point cloud completion. In *Proceedings of the AAAI Conference on Artificial Intelligence*, volume 39, 10689–10697.

Zhou, H.; Cao, Y.; Chu, W.; Zhu, J.; Lu, T.; Tai, Y.; and Wang, C. 2022. Seedformer: Patch seeds based point cloud completion with upsample transformer. In *Computer Vision—ECCV 2022: 17th European Conference, Tel Aviv, Israel, October 23–27, 2022, Proceedings, Part III*, 416–432. Springer.

Zhu, Z.; Chen, H.; He, X.; Wang, W.; Qin, J.; and Wei, M. 2023. SVDFormer: Complementing Point Cloud via Self-view Augmentation and Self-structure Dual-generator. In *Proceedings of the IEEE/CVF International Conference on Computer Vision*, 14508–14518.